

Overland water and salt flows in a set of rice paddies

by

Playán, E.¹*, Pérez-Coveta, O.¹, Martínez-Cob, A.¹, Herrero, J.²,
García-Navarro, P.³, Latorre, B.³, Brufau, P.³ and Garcés, J.³

Abstract

Cultivation of paddy rice in semiarid areas of the world faces problems related to water scarcity. This paper aims at characterizing water use in a set of paddies located in the central Ebro basin of Spain using experimentation and computer simulation. A commercial field with six interconnected paddies, with a total area of 5.31 ha, was instrumented to measure discharge and water quality at the inflow and at the runoff outlet. The soil was classified as a *Typic Calcixerept*, and was characterised by a mild salinity (2.5 dS m⁻¹) and an infiltration rate of 5.8 mm day⁻¹. The evolution of flow depth at all paddies was recorded. Data from the 2002 rice growing season was elaborated using a mass balance approach to estimate the infiltration rate and the evolution of discharge between paddies. Seasonal crop evapotranspiration, estimated with the surface renewal method, was 731 mm (5.1 mm day⁻¹), very similar to that of other summer cereals grown in the area, like corn. The irrigation input was 1,874 mm, deep percolation was 830 mm and surface runoff was 372 mm. Irrigation efficiency was estimated as 41%. The quality of surface runoff water was slightly degraded due to evapoconcentration and to the contact with the soil. During the period 2001-2003, the electrical conductivity of surface runoff water was 54% higher than that of irrigation water. However the runoff water was suitable for irrigation. A mechanistic mass balance model of inter-paddy water flow permitted to conclude that improvements in

¹ Departamento Suelo y Agua., Estación Experimental de Aula Dei, CSIC. P. O. Box 202. 50080 Zaragoza, Spain.

² Unidad de Suelos y Riegos, CITA, P.O Box 727, 50080 Zaragoza, Spain. Associated Unit to Estación Experimental de Aula Dei, CSIC.

³ Área de Mecánica de Fluidos, CPS, Universidad de Zaragoza. María de Luna, 3. 50018 Zaragoza, Spain.

* Corresponding author: playan@eead.csic.es; Phone: + 34 976 716 087; Fax: + 34 976 716 145.

27 irrigation efficiency can not be easily obtained in the experimental conditions. Since
28 deep percolation losses more than double surface runoff losses, a reduction in
29 irrigation discharge would not have much room for efficiency improvement.
30 Simulations also showed that rice irrigation performance was not negatively affected
31 by the fluctuating inflow hydrograph. These hydrographs are typical of turnouts
32 located at the tail end of tertiary irrigation ditches. In fact, these are the sites where rice
33 has been historically cultivated in the study area, since local soils are often saline-sodic
34 and can only grow paddy rice taking advantage of the low salinity of the irrigation
35 water. The low infiltration rate characteristic of these saline-sodic soils (an
36 experimental value of 3.2 mm day^{-1} was obtained) combined with a reduced irrigation
37 discharge resulted in a simulated irrigation efficiency of 60%. Paddy rice irrigation
38 efficiency can attain reasonable values in the local saline-sodic soils, where the
39 infiltration rate is clearly smaller than the average daily rice evapotranspiration.

40

41 **Keywords:** Ebro, Aragón, Spain, efficiency, simulation, saline-sodic, salinity,
42 infiltration, runoff, percolation

43 **Introduction**

44 In water-scarce regions of the world rice cultivation is often criticised for using too
45 much water. Tuong and Bhuiyan (1999) summarised the results of a number of
46 researchers in which rice irrigation efficiency fluctuated between 22 and 61%. These
47 results are in reasonable agreement with those of Clemmens and Dedrick (1994), who
48 presented a pessimistic and an optimistic estimation of paddy rice efficiency, with
49 respective values of 40 and 60%. According to these figures, it is clear that paddy rice
50 ranks very low in the comparison of irrigated agricultural systems based on irrigation
51 efficiency.

52 A number of authors (Keller et al., 1996; Perry, 1999) have emphasized the hydrologic
53 implications of irrigation efficiency, particularly in what refers to upscaling. A common
54 conclusion of these works is that low values of on-farm irrigation efficiency (Burt et al.,
55 1997) may not be harmful to regional water availability if the quality and location of
56 the return flows permit to reuse them. In fact, water reuse is a very common feature of
57 rice growing areas, in which water flows from paddy to paddy following intricate
58 paths. Recently, Hafeez et al. (2007) presented data on an irrigated rice project in the
59 Philippines. Water reuse at various levels resulted in a regional irrigation efficiency of
60 71%. The authors believed that achieving 80% efficiency would not require major
61 improvements in irrigation management and structures. Similar conclusions can be
62 drawn in the central Ebro basin of Spain when taking into account non point source
63 water reuse in the Flumen irrigation district (Nogués and Herrero, 2003). These
64 regional figures should alleviate social pressure on rice cultivation in areas where
65 return flows are reused.

66 The reduction of on-farm water use presents advantages over return flow reuse. These
67 are related to the conservation of water quantity (keeping irrigation water at the
68 system source; controlling watertable rise) and quality conservation (avoiding the
69 pollution present in runoff and percolation water). This is the reason why a number of
70 techniques have been proposed to improve on-farm rice irrigation efficiency, such as
71 soil puddling (Kukul and Aggarwal, 2002), intermittent ponding (Belder et al., 2004),
72 soil suitability assessment (Beecher et al., 2002) and nonsubmerged sprinkler irrigation
73 (McCauley, 1990).

74 The central Ebro Valley of Spain has an irrigated area of about half a million hectares.
75 The area cropped to rice fluctuates every year, but rarely exceeds 20,000 ha. Rice is not

76 particularly important in the region from a water use perspective, but it occupies its
77 own niche: it is the only cropping alternative for saline-sodic soils. The vertical
78 saturated hydraulic conductivity of these soils is usually very low, due to: 1) a
79 degraded structure; 2) the frequent alternating millimetric layers of silt and sodic clay
80 of the underlying Holocene sediments; and 3) soil tillage, puddling with the rice straw
81 to produce an impervious soil pan. As a consequence, rice irrigation can attain
82 reasonable efficiencies. In these crop conditions, soil salinity does not pose a limitation
83 to rice growth and yield due to the permanent flooding with fresh water. Saline-sodic
84 soils are often located in poorly drained, low geomorphic positions. Rice is cultivated
85 every year in these soils. In the years when rice is particularly profitable, the crop can
86 also be found in non saline-sodic soils occupying higher geomorphic positions. Rice
87 farms in the area often occupy between 3 and 10 ha, and are typically divided into a
88 number of paddies, with 0.5 to 2 ha each. The set of paddies has a canal turnout and a
89 runoff disposal point, and water continuously flows between paddies during the crop
90 season. Rainfall usually represents a small fraction of the seasonal water input.

91 The objectives of this paper are: 1) to assess water use in a set of rice paddies in the
92 central Ebro basin, estimating all terms of the hydrologic balance as well as irrigation
93 performance; 2) to evaluate the quality of irrigation and surface runoff waters; 3) to
94 assess the influence of soil infiltration on irrigation performance; and 4) to identify
95 better performing irrigation management techniques, capable of reducing surface
96 runoff.

97 **Material and Methods**

98 **The experimental field**

99 A commercial rice field located in *Albero Bajo* (Huesca, Ebro valley, Spain) was
100 evaluated in 2002 for irrigation performance and during 2001, 2002 and 2003 for
101 irrigation and runoff water quality. The coordinates of the field are 41° 59' 53" N and 0°
102 24' 34" W. The total field area was 5.31 ha, divided into six paddies with areas ranging
103 between 0.58 and 1.39 ha (Table 1, Figure 1). A topographic survey revealed that the
104 difference in elevation between the highest and the lowest paddies was 4.26 m. The
105 standard deviation of soil surface elevation (Playán et al., 1996) for each paddy ranged
106 between 0.010 and 0.021 m, indicating that the field had been laser-levelled in recent
107 years. Rice was grown annually in the field since 1996, following the attractive grain
108 prices and Common Agricultural Policy subsidies of the end of the 20th century. Rice
109 cultivation in the field was opportunistic, since according to the farmer other crops
110 could be successfully cultivated in the field.

111 The field was equipped with an underground low-pressure concrete pipeline for
112 surface irrigation water delivery to the six paddies. When used for rice irrigation the
113 irrigation system was modified by the farmer so that water could continuously run
114 from paddies 1 to 6. The concrete pipeline was only used to deliver water from the
115 irrigation ditch to paddy 1, from 2 to 3, and from 4 to 5. The rest of the connections
116 were performed using either the drainage system (1 to 2) or by breaching the paddy
117 dikes (from 3 to 4 and from 5 to 6). In this last case, a plastic sheet was used to line the
118 breach in order to prevent erosion. The connections between paddies were
119 continuously regulated by the farmer in order to maintain flow depth in the paddies at
120 target levels. The water levels and the regulations were performed in an empirical way.

121 During the 2002 season, the field was flooded on May 3. Rice sowing was performed
122 immediately after flooding (May 6), sprinkling the seed over the flooding water with a
123 fertilizer distributing machine. Physiological maturity was reached on September 23.
124 The cropping period involved the 143 days separating flooding from physiological
125 maturity.

126 **Characteristics of the climate and experimental soils**

127 The climate was characterized using the records of the nearby Grañén-Montesodeto
128 weather station. Mean annual temperature was 14.3°C, and mean annual precipitation
129 was 525 mm. The mean annual reference evapotranspiration (ET₀) was 1,304 mm (Faci
130 and Martínez-Cob, 1991). The soil temperature regime was classified as thermic (Soil
131 Survey Staff, 1999), while the soil moisture regime was xeric, according to the available
132 soil water holding capacity (Jarauta, 1989).

133 Mild soil salinity was evidenced by the abundant occurrence of *Tamarix sp.*, and
134 *Atriplex halimus* L. at the field berms. Some scarce *Suaeda vera* Forsskål ex J.F. Gmelin
135 could also be observed at the berms. The hydrophyte *Phragmites australis* (Cav.) Trin. ex
136 Steud. invaded the drainage ditches.

137 Several pits 2 m deep were dug to study the soil profile and for soil sampling,
138 following Schoenenberger et al. (2002). Electrical conductivity of the saturated paste
139 extract (ECe) was determined in all soil samples, as well as the major ions
140 concentration.

141 Mapping soil salinity at the experimental field was not considered necessary, since rice
142 development did not show irregularities. The average soil salinity was estimated using
143 electromagnetic induction (EMI) techniques. A hand-held EM38 sensor (Geonics Ltd.,
144 Mississauga, ON, Canada) was used at 101 points randomly distributed throughout
145 the field, resulting in a density of 19 reading points per ha. At each point
146 electromagnetic sensor readings were conducted in both the horizontal and vertical
147 dipole orientations, and soil elevation was determined using a radiometric total
148 station. The readings were corrected to the reference temperature of 25°C. After
149 dividing them by 100 to facilitate the calibration equations, the two corrected readings
150 were named EMh and EMv. Readings were converted to soil salinity by calibrating
151 against ECe determined in the soil samples taken by auger at 0-25 cm and 25-50 cm
152 depth at 16 locations immediately after each EMI reading. According to our experience
153 in nearby locations (Herrero et al., 2003; Nogués et al., 2006) a simple linear regression
154 was applied for calibration.

155 **Inflow-outflow water quality**

156 Water samples were collected at the inlet of paddy 1 (I1) and the outlet of paddy 6 (O6)
157 during the three experimental seasons. In each season, between 37 and 46 samples of

158 irrigation water and between 43 and 51 samples of surface runoff water were collected.
 159 The samples were analysed for electrical conductivity (at 25°C, EC), pH, major anions
 160 (Cl^- , SO_4^{2-} , HCO_3^- , CO_3^{2-}), major cations (Ca^{2+} , Mg^{2+} , Na^+ and K^+), and nutrients
 161 (nitrate and ammonia).

162 **Evapotranspiration estimation**

163 An automatic agrometeorological station was installed in paddy 5 (Figure 1). This
 164 station recorded half hour averages of the following variables: air temperature and
 165 relative humidity using a Vaisala probe HMP45AC; net radiation using a NR-Lite
 166 (Kipp & Zonen) net radiometer; soil heat flux using two HFP01 (Hukseflux) plates
 167 buried at 0.08 m depth; soil temperature at 0.03-0.06 m depth just above the soil heat
 168 flux plates using a TCAV (Campbell Scientific) probe; wind speed using a cup
 169 anemometer (A100R, Vector Instruments); and wind direction using a wind vane
 170 (W200P, Vector Instruments). High-frequency air temperature was also recorded with
 171 three fine-wire (76 μm diameter) thermocouples (chromel-constantan, TCBR, Campbell
 172 Scientific). These thermocouples were installed at 0.65, 1.40 and 2.15 m above ground,
 173 but were moved up as the crop grew in order to keep the lowest measurement height
 174 about 0.5 m above crop canopy. The cup anemometer, wind vane and Vaisala probe
 175 were kept at the same height as the highest thermocouple. The net radiometer was
 176 installed on a separate mast at 1.5 m above ground.

177 Rice evapotranspiration for half-hour periods was determined by solving the energy
 178 balance equation:

$$179 \quad \text{LE} = \text{Rn} - \text{G} - \text{H} \quad (1)$$

180 where: LE, latent heat flux; Rn, net radiation; G, soil heat flux; and H, sensible heat
 181 flux. All terms in Eq. (1) are expressed in W m^{-2} . Once determined, LE values were
 182 converted to evapotranspiration by using the following equation:

$$183 \quad \text{ET} = 1.8 \frac{\text{LE}}{\lambda} \quad (2)$$

184 where: ET, evapotranspiration expressed in mm (30 min)^{-1} ; λ is latent heat of
 185 vaporization (kJ kg^{-1}), computed from measured half-hour averages of air temperature
 186 as described elsewhere (Allen et al., 1998); and 1.8 is a unit conversion factor.

187 An additional term, the water heat storage, would have been included in Eq. (1)
 188 (Harazono et al., 1998). In this work, this term was neglected as irrigation water was
 189 permanently running over the paddy. In this situation changes in water temperature
 190 were mainly due to the convective transport heat by the running water rather than to
 191 the energy exchange between the surface and the atmosphere above it.

192 Soil heat flux at the soil surface was determined as follows (Allen et al., 1996):

$$193 \quad G = \frac{F1 + F2}{2} + \frac{\Delta T_s}{\Delta t} \rho_b d_z (840 + 4190\Theta) \quad (3)$$

194 where: F1 and F2, soil heat flux measured by the two plates buried at 0.08 m depth (W
 195 m⁻²); $\Delta T_s/\Delta t$ change in average soil temperature (°C) above the plates between two
 196 consecutive half-hour periods (thus, $\Delta t = 1800$ s); ρ_b , soil bulk density, 1,300 kg m⁻³, as
 197 determined from soil samples; d_z , burying depth of the soil heat flux plates, 0.08 m;
 198 and Θ , volumetric soil water content.

199 Sensible heat flux (H) was determined by the surface renewal method. This method
 200 was selected because it has been reported as a low-cost, low-maintenance, accurate
 201 method for ET determination (Snyder et al., 1996; Spano et al., 1997). Therefore it is
 202 appropriate when measurements along the whole crop season at remote places are
 203 required. This method is based on the fact that traces of high-frequency temperature
 204 data show ramp-like structures resulting from turbulent coherent structures (Paw U et
 205 al., 1992). Two parameters characterize these temperature ramps for unstable and
 206 stable atmospheric conditions (Paw U et al., 1992, 1995): the amplitude (a) and the
 207 inverse ramp frequency (ls). The mean values of these two parameters during a time
 208 interval (for instance, half-hour) can be used to estimate H over a vegetated surface
 209 using surface renewal (SR) analysis (Paw U et al., 1995; Snyder et al., 1996):

$$210 \quad H = \alpha \rho c_p \frac{a}{ls} z \quad (4)$$

211 where: ρ , moist air density (1.194 g m⁻³); c_p , specific heat of air (1.013 J g⁻¹ C⁻¹); z ,
 212 measurement height (m); α , a factor to account the effects of uneven temporal heat
 213 distribution in the canopy air and advective effects (Paw U et al., 1995); $\alpha = 1.0$ if the
 214 volume of air is heated evenly; measured values of α close to 1.0 have been reported
 215 when applying the surface renewal method over short canopies as long as
 216 measurements are taken well above crop canopy (Snyder et al., 1996; Spano et al.,

217 1997); thus, a value of $\alpha = 1.0$ was assumed in this paper. Three measurement heights
 218 were used for high-frequency air temperature readings in this work so three sets of H
 219 and corresponding ET values were computed through Eqs. (1), (2) and (4).

220 Snyder et al. (1996) and Spano et al. (1997) suggested use of the Van Atta (1977)
 221 approach to estimate the mean ramp characteristics used in Eq. (4). Thus, high-
 222 frequency temperature measurements were used to determine structure functions $S^n(r)$
 223 for each half-hour period according to the expression:

$$224 \quad S^n(r) = \frac{1}{m-j} \sum_{i=1+j}^m (T_i - T_{i-j})^n \quad (5)$$

225 where: m, number of data points measured at a frequency f (Hz) within a t-minute
 226 interval; n, function exponent (n = 2, 3 and 5), see Eq. (6) below; j, sample lag between
 227 data points corresponding to a time lag $r = j/f$; and T_i , the i^{th} temperature sample. In
 228 this work, t=30 min and f=0.25 s, thus m=7200; j=3; and r=0.75 s; values close to these
 229 have been reported as providing good results for short crops (Snyder et al., 1996; Spano
 230 et al., 1997; Zapata and Martínez-Cob, 2002).

231 The mean amplitude (a) for the 30-minute interval was estimated by solving the
 232 following equation for the real roots:

$$233 \quad a^3 + \left[10S^2(r) - \frac{S^5(r)}{S^3(r)} \right] a + 10S^3(r) = 0 \quad (6)$$

234 Finally, the inverse ramp frequency ls was calculated by the expression:

$$235 \quad ls = -\frac{a^3 r}{S^3(r)} \quad (7)$$

236 For a particular half-hour period and measurement height, the computed ls value was
 237 discarded if less than 5r (Snyder et al., 1996); in this case, H and LE estimates were not
 238 available. For a particular half-hour period, this problem rarely occurred
 239 simultaneously for the three measurement heights (only for 17 of 6,886 half-hour
 240 periods considered in this work). Because differences between LE estimates for the
 241 three measurement heights were small, as shown later, for a particular half-hour
 242 period, the average of the three LE estimates was computed in order to get a single LE
 243 estimate. The 17 unavailable data were estimated by linear interpolation between the
 244 two neighbouring half-hour periods.

245 **Flow depth and discharge measurements**

246 During the 2002 irrigation season, flow depth and discharge measurements were
247 performed in a number of points of the experimental field in order to characterize the
248 water balance. At the turnout of the irrigation ditch, a Cipolletti weir (Bos et al., 1984)
249 was installed. Discharge measurements at this point are representative of point I1 (see
250 Fig. 1). A V-shaped weir was installed at the field outlet, O6. Both weirs were
251 instrumented with shaft encoder level sensors and data loggers (OTT GmbH & Co.
252 Kempton, Germany). Both sensors produced continuous 30 min measurements of field
253 inflow and outflow.

254 Flow depth was manually recorded in all six paddies with an approximate frequency
255 of 4 days. The average of 17 soil surface elevation measurements per paddy were used
256 to establish the average soil surface elevation of each paddy. At each paddy, a
257 reference mark was established with an elevation equal to the average. All flow depth
258 measurements were referenced to these marks. In addition to manual measurements,
259 automatic measurements were performed at paddies 1 and 6. The previously reported
260 shaft encoder level sensors were used for this purpose. Automatic flow depth
261 measurements were taken every 30 min.

262 Measuring discharge between paddies was not an easy task. The critical-flow
263 conditions required to install weirs or flumes were only satisfied in O3 and O5.
264 Outflows O1, O2 and O4 used underground pipes, making it difficult to measure
265 discharge in a continuous fashion. Additionally, measuring devices would interfere
266 with the usual practices of the farmer, who continuously regulates these inter-paddy
267 structures. As a consequence, no additional structures were built to measure discharge.
268 A water balance method was used instead to estimate average discharge during certain
269 time intervals.

270 During the 2003 season, flow depth measurements were performed at the *Albero Bajo*
271 field and at a nearby rice field where the soil was saline-sodic. The new field was
272 located in *Callén* (Huesca, Ebro valley, Spain). The coordinates of the *Callén* field were
273 42°00'04"N and 0°22'04"W. In this season, the purpose of flow depth measurements
274 was to estimate soil infiltration. In both cases the procedure involved closing the inflow
275 and outflow of a paddy in each field and recording the evolution of flow depth during
276 the night time. Under the hypothesis that night evapotranspiration is negligible, the
277 decrease in flow depth can only be attributed to infiltration. In *Albero Bajo*, the

278 infiltration experiments were performed in the period June 9-12, and involved paddies
 279 1, 5 and 6. The abovementioned automatic flow depth recording instruments were
 280 used as in 2002. In *Callén* the experiment was performed from July 9 to 14. Flow depth
 281 was measured using an automatic shaft encoder level sensor.

282 **Water balance and irrigation performance**

283 Water balance in the experimental field between times t_1 and t_2 can be expressed in
 284 terms of volume as:

$$285 \quad \bar{I}(t_2 - t_1) + P A = ET A + DP A + \bar{O}(t_2 - t_1) + (S_2 - S_1) A \quad [8]$$

286 Where A is the field area, \bar{I} is average irrigation input discharge (determined at I1); P
 287 is precipitation; ET is evapotranspiration; DP is deep percolation rate; \bar{O} is average
 288 surface runoff output discharge (determined at O6); and $S_2 - S_1$ represents the change
 289 in overland storage as determined from flow depth measurements. The equation was
 290 applied to the whole field between the manual flow depth measurements of May 13th
 291 and September 23rd, and solved for the deep percolation rate (mm d^{-1}). Since in paddy
 292 rice the soil is saturated, deep percolation is equivalent to infiltration.

293 The water balance Eq. 8 was then used to estimate discharge between paddies. For this
 294 purpose, the equation was written for paddy j between two successive manual flow
 295 depth measurements, 1 and 2. In this case, the infiltration rate was an input to the
 296 equation:

$$297 \quad \bar{I}_j(t_2 - t_1) + P A_j = ET A_j + DP A + \bar{O}_j(t_2 - t_1) + (S_{j2} - S_{j1}) A_j \quad [9]$$

298 When equation 9 is successively applied to paddies 1 to 6 all intermediate average
 299 outflow discharges between times 1 and 2 can be estimated. The last outcome, \bar{O}_6 , can
 300 be contrasted with the measured value of field outflow, thus resulting in an error
 301 estimate. The equation can be equally run backwards from paddy 6 to 1 to estimate all
 302 intermediate average inflow discharges. In this case, the final outcome, \bar{I}_1 , can be
 303 compared with the field inflow and result in an error estimate. In this work the
 304 equation was solved in both directions, and the final discharge estimate for each paddy
 305 between two manual measurements was determined as the average of both forward
 306 and backward estimates.

307 Since there were 33 sets of flow depth recordings between May 13th and September
 308 23rd, a series of 32 discharge estimates were obtained for each paddy. The average flow

309 depth was determined for each paddy at each of the 32 time periods. Potential
 310 regressions were applied to each discharge - flow depth (h) data set to determine the
 311 seasonal discharge equations for each paddy:

$$312 \quad Q = p_{ij} h^{q_{ij}} \quad [10]$$

313 where p_{ij} and q_{ij} are the regression coefficients corresponding to discharge between
 314 paddies i and j. These regression equations represent the average conditions of each
 315 outflow throughout the 2002 season. It is important to stress that each of these
 316 equations do not represent the behaviour of a discharge structure at a point in time, but
 317 the “average” seasonal discharge law resulting from the frequent regulations
 318 performed by the farmer in the structure width, base elevation or opening.

319 Irrigation performance was estimated by the Irrigation efficiency (IE) term proposed by
 320 Burt et al. (1997), which can be expressed as:

$$321 \quad IE = \frac{\text{Volume of Irrigation Water Beneficially Used}}{\text{Volume of Irrigation Water Applied - Storage of Irrigation Water}} \quad [11]$$

322 The volume of irrigation water beneficially used was made equal to the volume of rice
 323 evapotranspiration.

324 **Simulation model for paddy flow**

325 A computer model was built to gain insight from the experimental results. The model
 326 simulates flow routing through the paddies using the previously discussed potential
 327 discharge equations. The model time step is adjustable: all required variables are
 328 linearly interpolated as needed. A time step of 30 min was used in all simulations in
 329 this work, in coincidence with the time step of variable input data. Model input
 330 includes field and paddy geometry, the time variation of irrigation inflow, ET and P,
 331 the infiltration rate and the parameters of the inter-paddy discharge equations. Model
 332 output includes the time variation of paddy flow depth and inter-paddy discharge, as
 333 well as all the terms of the water balance expressed in Eqs. 8 and 9 and the estimate of
 334 Irrigation Efficiency. The main simplifications used in the model are: a) soil surface
 335 elevation is considered constant inside each paddy, and microtopography does not
 336 affect the process of paddy filling and depleting; b) water movement in the paddies is
 337 slow, flow depth can be considered constant within a paddy, and water flow can be
 338 explained by mass conservation alone; and c) infiltration only occurs vertically and is
 339 not influenced by field boundaries.

340 During the simulated irrigation season, a paddy can eventually reach a zero flow
341 depth. In such case, the model responds by maintaining evapotranspiration
342 unchanged, and deducting this amount of water from deep percolation. It was
343 assumed that the paddy water table was shallow enough to fulfil crop water
344 requirements for a few days. This is not a valid hypothesis for long periods, in which
345 the crop would suffer from water stress.

346 Six simulation scenarios were designed to evaluate alternative irrigation conditions.
347 One of the simulation scenarios reproduced the experimental conditions, and served
348 the purpose of model validation. The remaining five scenarios were based on different
349 values of irrigation discharge and infiltration rate. Simulations were applied to the
350 complete crop season (from flooding to physiological maturity).

351 **Results and Discussion**

352 **Characteristics of the experimental soils**

353 Most soil samples in the pits and auger holes had loam or silty-loam texture, with few
354 coarse fragments of limestone. Calcium carbonate content was high in all samples,
355 according to the strong reaction to hydrochloric acid at 10% concentration. No
356 evidence of gypsum was found. A layer of massive structure occurred at a depth of
357 25 cm. This pan, about 15 cm thick, had signs of cycling between reduction and
358 oxidation conditions, with prevalence of the first ones; few straw residues were found,
359 however. Redoximorphic features did not occur in other layers of the studied profiles.
360 In April 5, 2001, before the seasonal flooding, the water table was found at 190 cm in
361 paddy 2 and at 110 cm in paddy 5. In some locations the densic pan underlied a C
362 horizon made by land levelling works, and was lying on a buried A horizon. Our
363 interpretation is that the densic layer results from repeated tillage of wet soil at the
364 same depth. The addition of rice straw to the puddling seems limited, in contrast with
365 other paddies in saline-sodic soils in depressed locations 1 km away from the
366 experimental farm.

367 Sodicity and salinity must be considered to understand the soil behavior. The soils in
368 the experimental field were moderately alkaline ($\text{pH} < 8.5$) and non-sodic, with $\text{SAR} <$
369 2 (Table 2), then chemical limitations to infiltration could be expected from the low
370 salinity of the irrigation water but not from soil sodicity. The ECe determined in
371 laboratory through the profiles was $< 2 \text{ dS m}^{-1}$, except the Ap horizon. This upper
372 horizon was more saline, with a median ECe value of 2.64 dS m^{-1} for 0-25 cm, and 3.72
373 dS m^{-1} for 25-50 cm in the samples taken at the 16 auger holes. Eleven of the 32 samples
374 taken by auger surpassed the 4 dS m^{-1} threshold for saline soils, all these saline samples
375 coming from the two lowest paddies. When ECe was computed for the 0-50 cm layer,
376 the median was 3.16 dS m^{-1} . The distribution of the values of ECe determined in
377 laboratory for the upper 50 cm of the soil along the paddies is shown with solid marks
378 in Figure 2.

379 EMh and EMv were linearly correlated, with $r = 0.990$. Notwithstanding, the regression
380 equations in Table 3 show that EMh (regression #1) performed better than EMv
381 (regression #2) in predicting ECe , both in terms of R^2 and the standard error of the
382 estimate. The parameters of the regression equations resulted very similar to those
383 previously obtained in the conterminous area of Barbués (Nogués et al., 2006) and

384 other close sites (Herrero et al., 2003). An exploratory data analysis of the distribution
385 of EMh and EMv found two groups of values: one for the paddies 1 to 4 and the other
386 for the paddies 5 and 6. These two lower paddies were much more saline than the rest,
387 as confirmed by the laboratory measurements of ECe represented by solid marks in
388 Figure 2.

389 In these circumstances, separate regressions were performed for paddies 1 to 4
390 (regressions #3 and #4) and for paddies 5 and 6 (regressions #5 and #6) (Table 3). EMv
391 performed better for the upper paddies, while EMh was the best choice for the lower
392 paddies. Therefore, we propose to use regressions #4 and #5 for the upper and lower
393 paddies, respectively. The different performance of EMh and EMv calibration in the
394 two groups of plots, as well as the low coefficients of determination and high standard
395 errors in regressions #5 and #6 can be attributed to the shallower water table in the
396 lower paddies. The ECe estimates, presented in Figure 2, showed a higher coefficient of
397 variation (Table 1) in the most saline paddies. The high coefficient of variation for the
398 entire experimental field (Table 1) was related with the differences in salinity between
399 higher and lower paddies.

400 The 101 estimates of ECe were represented against soil elevation in Figure 2 using
401 circles for the upper paddies and triangles for the lower paddies. These figures should
402 not be interpreted in terms of the physiological effects of soil salinity on the rice crop
403 because the rooting layer (about 0-25 cm) was less saline than the layer used for salinity
404 estimation (0-50 cm), and because of the low salinity of the flood water.

405 The mean (4.17 dS m^{-1}) and median (3.16 dS m^{-1}) of ECe determined in laboratory for
406 the 16 drilling points were in agreement with those calculated for the same points
407 either by a single calibration (regression #1, with 4.17 and 3.49 dS m^{-1} respectively) or
408 by separate calibrations (regressions #4 and #5, with 4.16 and 3.49 dS m^{-1} respectively).
409 When the 101 EMI readings were taken into account, a mean of 2.25 dS m^{-1} and a
410 median of 1.69 dS m^{-1} were obtained by single calibration, and a mean of 2.50 dS m^{-1}
411 and a median of 1.96 dS m^{-1} by separate calibrations. These figures confirmed the mild
412 salinity of the topsoil, whose mean of 2.50 dS m^{-1} is within the interval $2-4 \text{ dS m}^{-1}$ for
413 Very Slightly Saline soils (Schoenenberger et al. 2002), and agreed with the 1.94 dS m^{-1}
414 measured at the water table.

415 **Irrigation and runoff water quality**

416 The chemical characterisation of irrigation and runoff water is presented in Table 4.
417 Results were quite similar during the three years of study. This seems to be due to the
418 stable, low mineral load of the irrigation water, which is transported from the Pyrenees
419 through a network of mountain rivers and lowland canals. The years of continuous rice
420 cultivation add stability to the chemical properties of the runoff water. Due to this time
421 stability, average results from the three years of study will be discussed, with some
422 references to particular years.

423 The irrigation water electrical conductivity averaged 0.24 dS m^{-1} , with an inter annual
424 coefficient of variation of 22%. Runoff water averaged 0.37 dS m^{-1} . This increment in
425 salinity (54%) was significant, and could be attributed to two processes: 1) the
426 evapoconcentration of the irrigation water as it flows along the rice paddies; and 2) the
427 interaction with the saline soil. The experimental data did not allow us to establish the
428 relative importance of these processes. The salinity level of the runoff water was
429 compatible with its reuse for irrigation according to the guidelines of FAO (Ayers and
430 Wescot, 1984). In fact, this runoff water is currently mixed with drainage water and
431 reused for irrigation in the same project area. During its course over the rice field, the
432 pH of the water decreased from 8.2 to 7.5 (data from 2002), standing within the normal
433 range of 6.5-8.4 for irrigation waters. Regarding the major water ions, important
434 increases were seen in Cl^- (from 0.21 to $0.69 \text{ mmolc L}^{-1}$), and Na^+ (from 0.28 to 0.88
435 mmolc L^{-1}). Sodium chloride could be partly responsible for the increase in electrical
436 conductivity between irrigation and runoff water, agreeing with the presence of Na^+
437 and Cl^- in the soil profile (Table 2). The increment in SO_4^{2-} was moderate, in
438 coincidence with the absence of gypsum in the soil. The remaining ions did not show
439 significant increases.

440 Both irrigation and runoff water are of good quality in terms of crop use (Ayers and
441 Westcot, 1984). The load in nutrients is reasonable, in spite of the increase in both
442 ammonia and nitrates. Their respective levels do not raise environmental concerns but
443 contribute to the fertilization requirements of the crops that could be irrigated with this
444 water.

445 Regarding infiltration, according to the EC and SAR of the irrigation water, slight to
446 moderate use restrictions are expected. The runoff water falls in the class of no
447 restrictions, due to its increase in EC. The expected decrease in soil infiltration rate
448 produced by the irrigation water is not a problem, but an advantage for paddy rice.

449 **Evapotranspiration estimation**

450 The three sets of H values (one for each measurement height) provided slightly
451 different estimates of half-hour sensible heat. However, the average differences
452 between each other set of H values were low, -0.1 W m^{-2} between measurement heights
453 1 and 2, 1.1 W m^{-2} between measurement heights 1 and 3, and 1.2 W m^{-2} between
454 measurement heights 2 and 3. The corresponding root mean square errors were 29.1,
455 40.1 and 29.1 W m^{-2} , respectively. Regarding LE estimates, the differences between
456 measurement heights were similar, since the three sets of LE values were obtained
457 from Eq. (1) using the same R_n and G values. In terms of water depth, those root mean
458 square errors are equivalent to less than $0.03 \text{ mm (30 min)}^{-1}$. Therefore, the differences
459 in LE between the three measurement heights could be assumed to be negligible
460 (Figure 3).

461 Average rice evapotranspiration (ET) was 4.6 mm day^{-1} during May, and increased to
462 5.6 (June) and 6.4 mm day^{-1} (July) when the crop reached its maximum development;
463 the average rice ET then decreased to 5.3 in August and 3.5 mm day^{-1} in September
464 (Figure 4). The sharp decrease in ET during September was due to crop senescence,
465 which substantially reduced crop water requirements. Considering the period from
466 May 3 to September 23, total rice ET was 731 mm , a value similar to that of other
467 summer cereal crops grown in the area. This is the case of corn, a crop with sowing and
468 harvest dates similar to those of rice. Direct evaporation from the flooding water,
469 particularly at the early crop stages, is partly responsible for the similarity between rice
470 and corn seasonal ET.

471 Seasonal and daily rice ET values observed in this work were in general within the
472 lower limits of the ET rates reported in previous works (Shih et al., 1982; Mikkelsen
473 and DeDatta, 1991; Mohan and Arumugam, 1994; Harazono et al., 1998; Shah and
474 Edling, 2000). Rice ET has been reported to have great variability due to different
475 climatic conditions, management systems, rice varieties, etc. During the 2002 rice
476 season air temperatures were lower and precipitation was higher than long-term
477 averages (Figure 4). This was particularly true for July and August, so the atmospheric
478 evaporative demand was lower than in average years.

479 **Irrigation inflow and outflow**

480 Inflow to the field was very variable, as presented in Figure 5. This is not a rare finding
481 for a rice crop in the area. Water delivery in the irrigation district is based on an
482 arranged demand schedule, in which the flow rate is limited by the capacity of the
483 irrigation ditch, the irrigation duration is set to multiples of 24 hours, and the
484 frequency is negotiated between the farmer and the district personnel. Very often a
485 farmer completes irrigation before the end of the day and leaves the unused water in
486 the irrigation ditch. As previously discussed, rice is grown at low geomorphic
487 positions, which are also located at the end of the irrigation tertiary ditches. As a
488 consequence, rice farmers are the last water users in their tertiary, and receive very
489 fluctuating discharges. Rice farmers are useful to the irrigation districts, for it would
490 not be easy to use these uneven flows in other crops.

491 Figure 5 presents a reconstruction of the flooding period inflow based on the water
492 order filed by the farmer to the irrigation district. Two full days of water at a rate of
493 46.3 L s^{-1} (or $4,000 \text{ m}^3 \text{ d}^{-1}$, in the local farmers' units) were applied. This discharge was
494 out of the measuring range of the inflow weir. Therefore, water order data were used
495 in the Figure instead of flow measurements. During the cropping season the inflow
496 discharge equalled zero in a number of occasions. However, only one of these cases
497 was planned by the farmer: between June 11 and 16 the inflow was cut and the field
498 was completely emptied to apply herbicides. This is a common local practice known as
499 "*la seca*" (the dryout).

500 The field outflow was much smaller than the inflow, showed smooth patterns, and
501 responded to the peaks in inflow with a delay of 2-3 days. While the average post-
502 flooding inflow was 7.5 L s^{-1} , the average post-flooding outflow was 1.5 L s^{-1} .

503 **Flow levels in the paddies**

504 The time evolution of flow depth in all six paddies is presented in Figure 6. Continuous
505 data is presented for paddies 1 and 6 since the installation of the data loggers in May
506 24. Previous manual observations for these paddies are presented in dashed lines. The
507 flow level in paddy 1 reflected the variability of inflow discharge, and was much more
508 variable than flow level in paddy 6. Both paddies dried out during *la seca*: paddy 1
509 between June 16 and 17, and paddy 6 between June 16 and 19. It took five days for the
510 paddies to dry out after shutting off inflow. During the rest of the season, flow depth in
511 all paddies usually fluctuated between 0.06 and 0.14 m. This flow depth bracketed the
512 optimum value of 0.09 m, which was identified by Anbumozhi et al. (1998) for the

513 conditions of Japan in terms of paddy growth, production and water productivity. The
514 *Albero Bajo* farmer expressed that his target was 0.10 m. This target was successfully
515 obtained by a continuous regulation of the internal discharge structures. The farmer's
516 expertise and the large flooded area resulted in a relatively stable water regime in the
517 paddies despite the highly variable irrigation water supply flow rate.

518 **Water balance, irrigation performance and infiltration estimation**

519 Table 5 presents a seasonal field water balance. Input was dominated by irrigation:
520 1,874 mm. Seasonal precipitation was high for the location and period, but only
521 represented 8% of the irrigation input. As for the output, evapotranspiration was
522 second to deep percolation (731 and 830 mm, respectively). Surface runoff amounted to
523 372 mm, and finally storage resulted in 91 mm, which was the average final water
524 depth in the paddies. Deep percolation, obtained by balance closure, resulted in an
525 average infiltration rate of 5.8 mm d⁻¹.

526 Seasonal irrigation efficiency amounted to 41%. This figure compares well with the
527 values reported by Tuong and Bhuiyan (1999), and is on the low side of the estimates
528 provided by Clemmens and Dedrick (1994). A study performed by Lecina et al. (2007)
529 on the 125,000 ha of the *Riegos del Alto Aragón* irrigation project, where the
530 experimental field is located, concluded that the project wide irrigation efficiency for
531 2004 and 2004 averaged 78%. These results are similar to the findings by Hafeez et al.
532 (2007) for rice in the Philippines.

533 The infiltration experiments performed in 2003 using isolated paddies are based on the
534 hypothesis of negligible night time ET. The surface renewal night time ET estimations
535 performed in June and July 2002 in *Albero Bajo* yielded an average of -0.19 mm d⁻¹.
536 Since this estimated value was negative and small, it was considered negligible in the
537 context of infiltration estimation. The infiltration experiments yielded the following
538 results: 5.3 mm d⁻¹ in *Albero Bajo* and 3.2 mm d⁻¹ in *Callén*. Both sources of infiltration
539 data for *Albero Bajo* were quite coincident. The figure obtained from the field water
540 balance was retained because it was more time and space representative. Infiltration in
541 the saline-sodic soil of *Callén* was much lower than in *Albero Bajo*, owing to its
542 degraded structure and the underlying microlaminated sedimentary material. Both
543 infiltration rates are on the low range of the values reported by Bouman et al. (1994) for
544 a variety of rice soils and cultural practices. However, the infiltration rate of *Albero Bajo*

545 constituted the largest sink of irrigation water, and effectively controlled irrigation
546 performance.

547 **Estimation of inter-paddy discharge equations**

548 Figure 7 presents the derivation of parameters p and q in Eq. 10 for inter-paddy
549 discharge. While in some cases potential fit was adequate (O1 and O6, with respective
550 R^2 of 0.85 and 0.74), in other cases, such as O3 and O5, the regression model could not
551 explain 25% of the variability in discharge. In the case of parameter q , the estimated
552 values ranged from 0.94 to 3.2. As previously mentioned, outflow from paddy 6 was
553 recorded using a V-shaped weir. However, the farmer used his own structure
554 upstream from the weir to control outflow. Therefore, the equation for O6 corresponds
555 to the farmer's structure. The low coefficients of determination of the discharge
556 regressions can be attributed to the hydrological procedure used to derive pairs of
557 observations of head and discharge, and particularly, to the frequent structure
558 operations performed by the farmer to adjust paddy flow depth to his personal target.

559 **Scenario definition and simulation results**

560 The experimental results were used to build six simulation scenarios, characterized by
561 their discharge (Q) and infiltration (Z). Regarding discharge, all scenarios implemented
562 the flooding phase as designed by the farmer (8,000 m^3 applied in two days). For the
563 post-flooding discharge, two variables were used: the discharge can either be high
564 ("+", the experimental 7.5 L s^{-1}) or low ("-", 5.0 L s^{-1}); additionally, the discharge can be
565 variable ("v", proportional to the experimental variability) or uniform ("u"). For
566 infiltration there are two scenarios: high ("+", corresponding to *Albero Bajo*) and low
567 ("-", corresponding to *Callén*).

568 Scenario $Q_{hv}Z_h$ reproduces the experimental conditions, and was used to verify the
569 model. This scenario yielded adequate predictions of all hydrological seasonal
570 variables (Table 6). The simulated average flow depth in the experimental paddies was
571 0.094 m, which is compatible with flow depth measurements (Figure 6). Figure 8
572 presents scatter plots of observed and simulated semi hourly flow depth in paddies 1
573 and 6. The model successfully predicted flow depth in paddy 1, where most
574 observations are grouped along the 1:1 line. Regarding paddy 6, the situation was very
575 different. In fact, the observed flow depth in paddy 6 was usually in the narrow range
576 of 0.10 and 0.15 m (Fig. 5). Flow depth surpassed this range in two occasions, and went

577 down to zero during the dry out period (between June 17 and 20, in paddy 6). The
578 simulated values for flow depth in paddy 6 showed similar features to field
579 observations, but with significant time lags. For instance, the simulated dry out period
580 in paddy 6 lasted from June 21 to 29 (data not presented). This difference resulted in a
581 lack-of-fit to the 1:1 line in the low range of flow depth. Apparently, the farmer opened
582 the inter paddy structures to accelerate dry out, weed control treatment and refilling.
583 The procedure used in this work to estimate inter paddy discharge was not robust
584 enough to derive time-dependent discharge coefficients for each paddy outflow. In any
585 case, a large proportion of paddy 6 flow depth observations followed the 1:1 line.

586 The different simulation scenarios provided answers to irrigation management
587 questions. The comparison between simulation results for $Q+vZ+$ and $Q+vZ+$
588 indicated that if the farm was located in a saline-sodic soil (low infiltration) and the rest
589 of conditions was kept constant, the reduction in deep percolation would be
590 compensated by an increase in surface runoff losses. In order to convey more overland
591 flow, depth would increase from an average 0.094 m to 0.113 m (Table 6). As a result,
592 efficiency would remain basically unchanged. Scenarios $Q+cZ+$ and $Q+cZ-$ can be
593 compared to their variable discharge parallels, to conclude that the use of highly
594 variable irrigation water supply has very little impact on irrigation performance and
595 on the hydrological balance. As a consequence, it can be stated that in this particular
596 case rice irrigation does not pay a price for using a typical tail-end hydrograph. Of
597 course this last sentence only considers the irrigation water use perspective. A number
598 of agronomic traits could be affected by a strong variability in irrigation water input.
599 The last two scenarios explored the reduction in post-flooding irrigation discharge.
600 Simulation of $Q-cZ+$ resulted in extended dry periods for the downstream paddies. For
601 instance, paddies 5 and 6 remained dry after mid June. As a consequence, reducing
602 irrigation discharge was not a viable procedure to increase efficiency in the
603 experimental farm. The water balance sinks were dominated by deep percolation, and
604 reducing the moderate surface runoff losses induced risks of crop failure. Finally,
605 scenario $Q-cZ-$ showed that in saline-sodic soils (low infiltration), a low post-flooding
606 irrigation discharge can be successfully used to boost irrigation efficiency to 60%. Even
607 in these low-infiltration conditions, deep percolation losses constitute a major loss of
608 water.

609 Conclusions

- 610 • In the experimental conditions surface runoff amounted to 18.3% of the seasonal
611 water input (irrigation plus precipitation). The quality of surface runoff water was
612 slightly deteriorated by rice cultivation, with a 0.13 dS m⁻¹ (53%) increase in
613 electrical conductivity. This could be explained by two processes: the
614 evapoconcentration of the irrigation water and the uptake of soil sodium chloride
615 during water flow along the paddies. The overall quality of surface runoff water
616 was good enough for its reuse for irrigation without restrictions.
- 617 • A significant part of the irrigation input (41.0%) was lost to deep percolation. The
618 complex interaction between the percolating water and the seasonal shallow water
619 table typical of rice cultivated areas prevented us from evaluating the quality of
620 deep percolation water in this work. The reported water balance indicates that the
621 environmental sustainability of rice cultivation heavily depends on this issue.
- 622 • Current irrigation efficiency in the experimental field, 41%, is in line with previous
623 findings for paddy rice. The seasonal consumptive water use (ET), 731 mm, was
624 similar to that of other summer cereals grown in the area, like corn.
- 625 • Rice cultivation at the experimental farm does not allow substantial improvements
626 in irrigation efficiency through the adjustment of discharge, as most losses are due
627 to infiltration. Using a lower irrigation discharge would result in reduced runoff.
628 However, flow depths would be smaller, and —besides possible agronomic effects—
629 accurate land levelling and intense surveillance would be required to ensure that
630 all parts of the fields were covered with water throughout the season. The
631 improvement of irrigation efficiency in the experimental farm could be obtained by
632 irrigation management techniques such as intermittent ponding or soil puddling.
- 633 • Simulations showed that irrigation performance did not substantially improve for a
634 uniform post-flooding irrigation discharge (irrigation efficiency of 42%). Paddy rice
635 cultivation was not affected by the variability of the inflow hydrograph. In the
636 experimental area, where rice is generally cultivated in saline-sodic soils located at
637 the low, downstream end of irrigation tertiary ditches, this is the only feasible crop.
638 Its irrigation performance is not affected by the fluctuating irrigation discharge
639 typical of a canal tail end.

640 • Simulated irrigation efficiency increased from 41% to 60% when infiltration was
641 decreased from 5.8 to 3.2 mm day⁻¹ and the post flooding irrigation discharge was
642 reduced from 7.5 to 5.0 L s⁻¹. Saline-sodic soils can provide increased irrigation
643 efficiency through the control of deep percolation losses. This control is achieved
644 through saline-sodic soils inherent low infiltration, which is accentuated by soil
645 puddling. Soil infiltration therefore is a major control variable to assess the
646 suitability of a soil for paddy rice cultivation. A decrease in percolation losses from
647 832 to 459 mm, as shown here, will result in reduced water losses and a reduction
648 in deep percolation pollutant loads, thus contributing to the sustainability of paddy
649 rice cultivation in the conditions of the central Ebro valley of Spain.

650 **Acknowledgements**

651 This research was funded by the *Plan Nacional de I+D+i* of the Government of Spain,
652 through grant AGL2000-1775. Olga Pérez Coveta received a scholarship from the *Plan*
653 *Nacional de Formación de Personal Investigador* of the Government of Spain. We are very
654 grateful to José María Arnal, the *Albero Bajo* farmer, for his cooperation throughout the
655 experiments. Finally, it would have been impossible to complete this work without the
656 enthusiastic support from our field team: Miguel Izquierdo, Jesús Gaudó and Daniel
657 Mayoral.

658 **References**

- 659 Allen, R.G., Pruitt, W.O., Businger J.A. 1996. Evapotranspiration and Transpiration. In:
660 Hydrology Handbook (2nd ed.). Heggen R.J., Wootton T.P., Cecilio C.B., Fowler
661 L.C., Hui S.L. (eds). 125-252. American Society of Civil Engineers. New York, NY,
662 USA.
- 663 Allen, R.G., Pereira, L.S., Raes D., Smith M. 1998. Crop evapotranspiration: guidelines
664 for computing crop water requeriments. FAO Irrigation and Drainage Paper 56.
665 FAO, Rome, Italy.
- 666 Anbumozhi, V, Yamaji, E., Tabichhi, T. 1998. Rice crop growth and yield as influenced
667 by changes in ponding water depth, water regime and fertigation level. *Agric. Wat.*
668 *Manage.*, 37(3): 241-253.
- 669 Ayers, R.S., Westcot, D.W. 1984. Water quality for agriculture. FAO Irrigation and
670 Drainage Paper, 29 Rev. 1. Reprinted 1989, 1994. FAO, Rome.
- 671 Beecher, H.G., Hume, I.H., Dunn, B.W. 2002. Improved method for assessing rice soil
672 suitability to restrict recharge. *Australian Journal of Experimental Agriculture*, 42
673 (3): 297-307.
- 674 Belder, P., Bouman, B.A.M., Cabangon, R., Guían, L., Quilang, E.J.P., Yuanhua, L.,
675 Spiertz, J.H.J., Tuong, T.P. 2004. Effect of water-saving irrigation on rice yield and
676 water use in typical lowland conditions in Asia. *Agric. Wat. Manage.*, 65(3): 193-210.
- 677 Bos, M.G., Replogle, J.A., Clemmens, A.J. 1984, Flow measuring flumes for open
678 channel systems: New York, USA, John Wiley & sons, Inc.
- 679 Bouman, B.A.M., Wopereis, M.C.S., Kropff, M.J., ten Berge, H.F.M., Tuong, T.P. 1994.
680 *Agric. Wat. Manage.*, 26(4): 291-304.
- 681 Burt, C.M., Clemmens, A.J., Strelkoff, T.S., Solomon, K.H., Bliesner, R.D., Hardy. L.,A.,
682 Howell, T.A., Eisenhauer, D.E. 1997. Irrigation performance measures: efficiency
683 and uniformity. *J. Irrig. Drain. Div.*, ASCE, 123(6), 423-442.
- 684 Clemmens, A.J., Dedrick, A.R., 1994. Irrigation techniques and evaluations. In: K.K.
685 Tanji, B. Yaron (Eds.), *Adv. series in agricultural sciences*. Springer-Verlag, Berlin,
686 pp. 64-103.
- 687 Faci, J.M., Martínez-Cob, A. 1991. Cálculo de la evapotranspiración de referencia en
688 Aragón. Departamento de Agricultura. Gobierno de Aragón. Zaragoza, Spain.

- 689 Hafeez, M.M., Bouman, B.A.M., Van de Giesen, N., Vlek, P. 2007. Scale effects on water
690 use and water productivity in a rice-based irrigation system (UPRIIS) in the
691 Philippines. *Agric. Wat. Manage.*, 92(1-2): 81-89.
- 692 Harazono Y., Kim J., Miyata A., Choi T., Yun J.I., Kim J.W. 1998. Measurement of
693 energy budget components during the International Rice Experiment (IREX) in
694 Japan. *Hydrological Processes*. 12: 2081-2092.
- 695 Herrero, J., Ba, A.A., Aragüés, R. 2003. Soil salinity and its distribution determined by
696 soil sampling and electromagnetic techniques. *Soil Use and Management*. 19(2):
697 119-126.
- 698 Jarauta, E. 1989. Modelos matemáticos de régimen de humedad del suelo. PhD Thesis,
699 Universidad Politécnica de Barcelona, Spain.
- 700 Keller, A., Keller, J., Seckler, D. 1996. Integrated water resource systems: Theory and
701 policy implications. Research Report 3. Colombo, Sri Lanka: International Irrigation
702 Management Institute (IIMI).
- 703 Kukal, S.S., Aggarwal, G.C. 2002 Percolation losses of water in relation to puddling
704 intensity and depth in a sandy loam rice (*Oryza sativa*) field. *Agric. Wat. Manage.*,
705 57(1): 49-59.
- 706 Lecina, S., Zapata, N., Playán, E., Salvador, R., Faci, J.M., Mantero, I., Cavero, J.,
707 Andrés, J. 2007. Consecuencias de la modernización del regadío sobre el
708 aprovechamiento del agua en Riegos del Alto Aragón. XXV Congreso Nacional de
709 Riegos. Comité Español de Riegos y Drenajes. Pamplona, Spain.
- 710 McCauley, G.N. 1990. Sprinkler vs. Flood Irrigation in Traditional Rice Production
711 Regions of Southeast Texas. *Agronomy Journal*, 82(4): 677-682.
- 712 Mikkelsen D.S., DeDatta S.K. 1991. Rice culture. In: Rice production. Luh B.S. (ed.). Vol.
713 1: 103-186. Van Nostrand Reinhold. New York, NY, USA.
- 714 Mohan S., Arumugam N. 1994. Irrigation crop coefficients for lowland rice. *Irrig. and
715 Drain. Sys.* 8: 159-176.
- 716 Nogués, J., Herrero, J. 2003. The impact of transition from flood to sprinkling irrigation
717 on water district consumption. *Journal of Hydrology* 276: 37-52.
- 718 Nogués, J., Robinson, D.A., Herrero, J. 2006. Incorporating electromagnetic induction
719 methods into regional soil salinity survey of irrigation districts. *Soil Science Society
720 of America Journal* 70: 2075-2085.

- 721 Paw U, K.T., Brunet, Y., Collineau, S., Shaw, R.H., Maitani, T., Qiu, J., Hipps, L. 1992.
722 On coherent structures in turbulence above and within agricultural plant canopies.
723 *Agric. For. Meteorol.* 61: 55-68.
- 724 Paw U, K.T., Qiu, J., Su, H.B., Watanabe, T., Brunet Y. 1995. Surface renewal analysis: a
725 new method to obtain scalar fluxes without velocity data. *Agric. For. Meteorol.* 74:
726 119-137.
- 727 Perry, C.J., 1999. The IWMI water resources paradigm - definitions and implications.
728 *Agric. Wat. Manage.*, 40, 45-50.
- 729 Playán, E., Faci, J.M., Serreta, A. 1996, Modeling microtopography in basin irrigation. *J.*
730 *Irrig. Drain. Div., ASCE*, 122(6): 339-347.
- 731 Schoenenberger, P.J., Wysocki, D.A., Benham, E.C., Broderson, W. D. (Eds.) 2002. Field
732 book for describing and sampling soils, Version 2.0. Natural Resources
733 Conservation Service, National Soil Survey Center, Lincoln, NE.
- 734 Shah, S.B., Edling, R.J. 2000. Daily evapotranspiration prediction from Louisiana
735 flooded rice field. *J. Irrig. Drain. Div., ASCE*, 126 (1): 8-13.
- 736 Shih, S.F., Rahi, G.S., Harrison, D.S. 1982. Evapotranspiration studies on rice in relation
737 to water use efficiency. *Trans. ASAE.* 25(3): 702-707, 712.
- 738 Snyder, R.L., Spano, D., Paw U, K.T. 1996. Surface renewal analysis for sensible and
739 latent heat flux density. *Bound.-Layer Meteorol.* 77: 249-266.
- 740 Soil Survey Staff. 1999. *Soil Taxonomy*. 2nd ed. Natural Resources Conservation Service,
741 Agriculture Handbook 436. USDA. Washington D.C.
- 742 Spano, D., Snyder, R.L., Duce, P., Paw U, K.T. 1997. Surface renewal analysis for
743 sensible heat flux density using structure functions. *Agric. For. Meteorol.* 86: 259-
744 271.
- 745 Tuong, T.P., Bhuiyan, S.I. 1999. Increasing water-use efficiency in rice production:
746 farm-level perspectives. *Agric. Wat. Manage.*, 40(1): 117-122.
- 747 Van Atta, C.W. 1977. Effect of coherent structures on structure functions of
748 temperature in the atmospheric boundary layer. *Archives of Mechanics.* 29 (1): 161-
749 171.
- 750 Zapata, N., Martínez-Cob, A. 2002. Evaluation of the surface renewal method to
751 estimate wheat evapotranspiration. *Agric. Wat. Manage.* 55 (2): 141-157.

752 **List of Tables**

753 **Table 1.** *Main characteristics of the paddies: area (m²), average soil surface elevation (m,*
 754 *referenced to paddy 6), standard deviation of soil surface elevation (SDe, m), number of EMI*
 755 *readings, and statistics of the ECe 0-50 cm estimates.*

756 **Table 2.** *Saturation percentage (SP) and chemical characterization of the saturation extract*
 757 *from soil samples obtained from pit "Albero Bajo 4", described in 29/4/2001 in paddy 2. The soil*
 758 *was classified as a fine-loamy, mixed, calcareous, thermic, Typic Calcixerept (Soil Survey Staff,*
 759 *1999).*

760 **Table 3.** *Simple linear regressions of ECe (dS m⁻¹) determined in the laboratory in soil samples*
 761 *from 0 to 50 cm depth taken at 16 drilling points, on the EMI readings (EMh or EMv) in these*
 762 *points. Regression parameters are accompanied by the coefficient of determination, R² (%), and*
 763 *the standard error of the estimate, S.*

764 **Table 4.** *Chemical characterization of the irrigation and runoff water in the set of rice paddies*
 765 *for the years 2001, 2002 and 2003, and for the average of the three years. Number of samples*
 766 *(n), mean and coefficient of variation (CV, %) are provided for electrical conductivity, pH and*
 767 *for the concentration of ions and nutrients. The table also includes the Na⁺/ Ca²⁺ ratio and the*
 768 *Sodium Adsorption Ratio (SAR).*

769 **Table 5.** *Elements of crop water balance in the set of paddies as measured in 2002. Water*
 770 *balances were established from flooding to physiological maturity (from May 3 to September*
 771 *23).*

772 **Table 6.** *Hydrologic characterisation and irrigation performance observed in 2002 and*
 773 *simulated with the model. The flooding volume, applied during two days before sowing, was the*
 774 *same in all cases (8,000 m³). Simulations were performed between flooding and physiological*
 775 *maturity. Simulated and observed post-flooding average discharges refer to the period May 5 to*
 776 *September 23. The post-flooding simulated discharge may be constant or variable. Variable*
 777 *discharge was equal to the observed discharge. Uniform discharge was kept constant after*
 778 *flooding.*

779 **Table 1.** *Main characteristics of the paddies: area (m²), average soil surface elevation (m,*
 780 *referenced to paddy 6), standard deviation of soil surface elevation (SDe, m), number of EMI*
 781 *readings, and statistics of the ECe 0-50 cm estimates.*

782

Paddy #	Area (m ²)	Elevation (m)	SDe (m)	EMI readings	ECe 0-50 cm estimates				
					Mean (dS m ⁻¹)	Median (dS m ⁻¹)	Min. (dS m ⁻¹)	Max. (dS m ⁻¹)	C.V. (%)
1	7,973	4.26	0.021	17	1.53	1.43	1.07	2.09	22.2
2	10,004	2.57	0.010	20	1.32	1.26	0.92	2.05	24.2
3	5,844	1.62	0.019	10	1.44	1.43	1.05	1.71	16.0
4	7,188	0.99	0.020	15	1.86	1.69	1.15	3.40	37.1
5	8,240	0.26	0.019	21	4.68	4.31	2.49	9.86	46.2
6	13,866	0.00	0.014	18	3.31	2.69	2.10	8.56	48.6
All	53,115	-	0.017	101	2.50	1.96	0.92	9.86	71.6

783

784 **Table 2.** Saturation percentage (SP) and chemical characterization of the saturation extract
 785 from soil samples obtained from pit "Albero Bajo 4", described in 29/4/2001 in paddy 2. The soil
 786 was classified as a fine-loamy, mixed, calcareous, thermic, Typic Calcixerept (Soil Survey Staff,
 787 1999).

788

Depth (cm)	SP (%)	pH (-)	ECe (dSm ⁻¹)	Ca ²⁺ (mmolc L ⁻¹)	Mg ²⁺ (mmolc L ⁻¹)	Na ⁺ (mmolc L ⁻¹)	SAR (mmolc L ⁻¹) ^{0.5}	CO ₃ H ⁻ (mmolc L ⁻¹)	SO ₄ ²⁻ (mmolc L ⁻¹)	Cl ⁻ (mmolc L ⁻¹)	NO ₃ ⁻ (mmolc L ⁻¹)
0-20	36	8.27	1.20	9.10	1.77	1.47	0.6	3.0	7.96	1.90	0.04
20-40	33	8.38	0.60	3.32	1.15	1.23	0.8	2.2	1.41	0.92	1.41
40-60	34	8.35	0.47	1.85	1.00	1.21	1.0	1.6	1.41	0.92	1.41
60-80	30	8.43	0.53	2.41	1.16	1.43	1.1	1.6	2.43	1.01	0.04
80-100	29	8.37	0.58	2.22	1.18	1.73	1.3	1.8	2.75	1.17	0.26
100-120	31	8.24	0.65	4.55	2.76	3.49	1.8	1.4	3.28	1.25	2.63
120-140	31	8.27	0.66	1.81	1.17	2.19	1.8	1.6	3.20	1.44	0.41
140-160	32	8.33	0.65	1.72	1.21	2.29	1.9	1.8	3.04	1.47	0,47

789

790 **Table 3.** Simple linear regressions of E_{Ce} (dS m⁻¹) determined in the laboratory in soil
 791 samples from 0 to 50 cm depth taken at 16 drilling points, on the EMI readings (EMh or
 792 EMv) in these points. Regression parameters are accompanied by the coefficient of
 793 determination, R² (%), and the standard error of the estimate, S.

794

Paddies	EMI reading	Regression #	E _{Ce} = a + b EMI			
			*a (dS m ⁻¹)	**b (-)	R ² (%)	S (dS m ⁻¹)
All	EMh	1	-0.043	3.67 (0.53)	77.6	1.50
	EMv	2	-0.121	3.01 (0.54)	68.7	1.78
1 to 4	EMh	3	0.602	2.15 (0.44)	79.9	0.46
	EMv	4	0.632	1.59 (0.31)	81.3	0.44
5 and 6	EMh	5	0.933	3.31 (1.07)	61.6	2.03
	EMv	6	1.113	2.65 (1.13)	47.9	2.37

795

(*) these values do not differ from 0 significantly (P = 0.05);

796

(**) the standard error of b is in parenthesis.

797 **Table 4.** Chemical characterization of the irrigation and runoff water in the set of rice paddies
 798 for the years 2001, 2002 and 2003, and for the average of the three years. Number of samples
 799 (n), mean and coefficient of variation (CV, %) are provided for electrical conductivity, pH and
 800 for the concentration of ions and nutrients. The table also includes the Na⁺/ Ca²⁺ ratio and the
 801 Sodium Adsorption Ratio (SAR).

802

Year		2001		2002		2003		2001-2003		
Kind of water		Irrigation	Runoff	Irrigation	Runoff	Irrigation	Runoff	Irrigation	Runoff	
Electrical conductivity (EC, dS m ⁻¹)	n	8	14	11	12	18	17	37	43	
	Mean	0.26	0.33	0.27	0.5	0.18	0.29	0.24	0.37	
	CV	13	16	9	26	43	50	22	31	
pH	n	0	0	11	12	0	0	11	12	
	Mean	-	-	8.2	7.5	-	-	8.2	7.5	
	CV	-	-	2	2	-	-	2	2	
Major anions* (mmolc L ⁻¹)	Cl ⁻	n	8	14	20	20	18	17	46	51
		Mean	0.26	0.61	0.12	0.67	0.24	0.78	0.21	0.69
		CV	40	39	71	114	73	76	61	76
	SO ₄ ²⁻	n	8	14	20	20	18	17	46	51
		Mean	0.57	0.61	0.31	0.41	0.46	0.56	0.45	0.53
		CV	11	40	63	123	42	79	39	81
	HCO ₃ ⁻	n	8	14	20	20	18	17	18	17
		Mean	ip	ip	ip	ip	1.27	1.63	1.27	1.63
		CV	-	-	-	-	58	78	58	78
Major cations (mmolc L ⁻¹)	Ca ²⁺	n	8	14	16	17	18	17	42	48
		Mean	1.16	1.09	0.75	0.99	0.83	1.03	0.91	1.04
		CV	7	31	64	74	77	96	49	67
	Mg ²⁺	n	8	14	14	18	18	17	40	49
		Mean	0.58	0.78	0.39	0.61	0.67	0.78	0.55	0.72
		CV	14	15	36	65	42	41	31	40
	Na ⁺	n	8	14	16	19	18	17	42	50
		Mean	0.30	0.72	0.18	0.96	0.35	0.97	0.28	0.88
		CV	40	39	34	88	65	59	46	62
	K ⁺	n	8	14	20	20	18	17	46	51
		Mean	0.06	0.06	0.03	0.03	0.06	0.13	0.05	0.07
		CV	37	47	55	72	70	81	54	67
Na ⁺ / Ca ²⁺ ratio		0.26	0.66	0.24	0.97	0.43	0.93	0.30	0.85	
SAR from the above means of Na ⁺ , Ca ²⁺ and Mg ²⁺		0.3	0.7	0.2	1.1	0.4	1.0	0.3	0.9	
Nutrients (mg L ⁻¹)	NO ₃ ⁻	n	5	3	5	1	5	0	15	4
		Mean	0.3	3.6	0.1	1.1	3.4	-	1.27	2.35
		CV	46	131	51	0	55	-	51	66
	NH ₄ ⁺	n	0	2	15	6	7	6	22	14
		Mean	-	3.1	0.2	0.5	0.4	0.9	0.3	1.5
		CV	-	6	45	79	35	95	40	60

(*) CO₃²⁻ was inappreciable (concentration below the detection threshold of the laboratory equipment) in all samples.

(ip) Inappreciable.

803

804 **Table 5.** *Elements of crop water balance in the set of paddies as measured in 2002. Water*
 805 *balances were established from flooding to physiological maturity (from May 3 to September*
 806 *23).*

807

		Volume	Depth	Volume or Depth
		(m ³)	(mm)	(%)
Input	Irrigation	99,516	1,874	92.6
	Precipitation	7,973	150	7.4
	Total input	107,488	2,024	100.0
Output	Evapotranspiration	38,820	731	36.1
	Deep percolation	44,080	830	41.0
	Overland storage	4,818	91	4.5
	Runoff	19,771	372	18.4
	Total output	107,488	2,024	100.0

808

809

810 **Table 6.** *Hydrologic characterisation and irrigation performance observed in 2002 and*
 811 *simulated with the model. The flooding volume, applied during two days before sowing, was the*
 812 *same in all cases (8,000 m³). Simulations were performed between flooding and physiological*
 813 *maturity. Simulated and observed post-flooding average discharges refer to the period May 5 to*
 814 *September 23. The post-flooding simulated discharge may be constant or variable. Variable*
 815 *discharge was equal to the observed discharge. Uniform discharge was kept constant after*
 816 *flooding.*

817

	Variable	Observed	Simulation Scenario					
			Q+vZ+	Q+vZ-	Q+cZ+	Q+cZ-	Q-cZ+	Q-cZ-
Scenario definition	Post-flooding average	7.5	7.5	7.5	7.5	7.5	5.0	5.0
	Irrigation discharge (L s ⁻¹)							
	Infiltration rate (mm d ⁻¹)	5.8	5.8	3.2	5.8	3.2	5.8	3.2
Hydrological balance	Irrigation (mm)	1,874	1,874	1,874	1,877	1,877	1,301	1,301
	Deep percolation (mm)	830	832	459	832	459	624	459
	Final overland storage (mm)	91	101	117	115	131	0	82
	Runoff (mm)	372	360	717	349	705	97	179
	Irrigation efficiency (%)	41	41	42	41	42	56	60
	Average simulated flow depth (m)	-	0.094	0.113	0.096	0.115	0.050	0.062

818

819 **List of Figures**

820 **Figure 1.** *Set up of the field experiment, showing the location of the six paddies, the irrigation*
 821 *ditch and the open drain, the irrigation water course, the agrometeorological station and the*
 822 *inflows and outflows of each paddy (for paddy i , I_i and O_i , respectively).*

823 **Figure 2.** *Estimates of E_{c_e} from 0 to 50 cm in the 101 EMI reading points (open marks) and*
 824 *laboratory measured E_{c_e} up to the same depth in 16 of these points (solid marks), against their*
 825 *relative elevation. Calibration in paddies 1 to 4 (circles) was performed with regression #4, and*
 826 *in paddies 5 and 6 (triangles) with regression #5 (see Table*

827 **Figure 3.** *Half-hour LE estimates obtained for measurement height 1 (0.5 m above crop canopy,*
 828 *x -axis) versus half-hour LE estimates obtained for measurement heights 2 and 3 (0.75 and 1.5*
 829 *m above measurement height 1, respectively) (y -axis).*

830 **Figure 4.** *Seasonal evolution of crop evapotranspiration estimates and precipitation*
 831 *measurements.*

832 **Figure 5.** *Seasonal evolution of field irrigation inflow (I_1) and runoff (O_6). The inflow during*
 833 *May 5 and 6 served the purpose of flooding the field. Since the discharge was out of the range of*
 834 *the measuring device, its value was taken from the farmer water order to the irrigation district.*

835 **Figure 6.** *Seasonal evolution of measured flow depth in the paddies. Flow depth was*
 836 *automatically measured every 30 min in paddies 1 and 6 and manually measured in paddies 2,*
 837 *3, 4 and 5. Automatic recording started in May 24. Previous values for paddies 1 and 6 were*
 838 *manually measured (dashed line).*

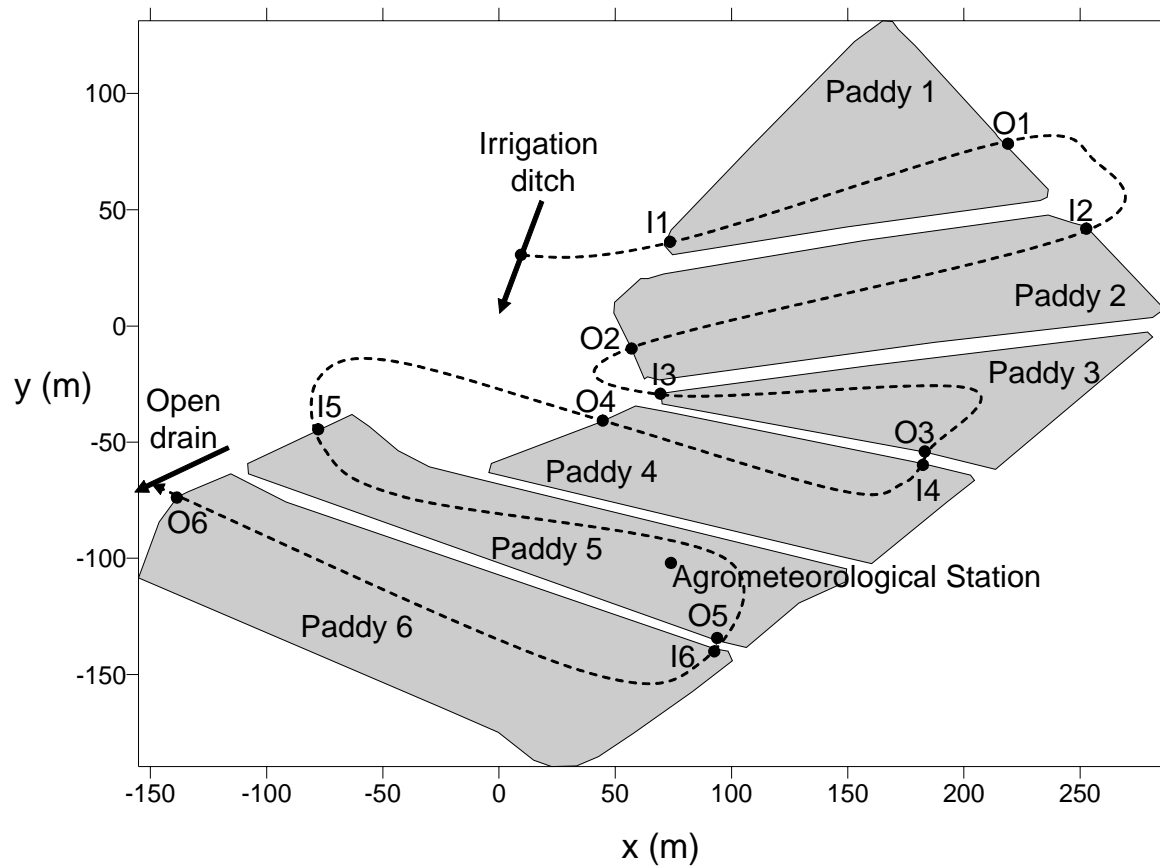
839 **Figure 7.** *Inter-paddy seasonal flow depth-discharge relationships. Scatter plots, potential*
 840 *regression lines, regression equations and coefficients of determination are presented for*
 841 *outflows from paddies 1 to 6.*

842 **Figure 8.** *Observed vs. simulated values of flow depth in paddies 1 (a) and 6 (b).*

843 **Figure 9.** *Time evolution of flow depth in Paddy 3 as observed and as simulated for scenarios*
 844 *$Q+vZ+$, $Q+vZ-$, $Q+cZ+$ and $Q-cZ-$.*

845 **Figure 1.** Set up of the field experiment, showing the location of the six paddies, the irrigation
 846 ditch and the open drain, the irrigation water course, the agrometeorological station and the
 847 inflows and outflows of each paddy (for paddy i , I_i and O_i , respectively).

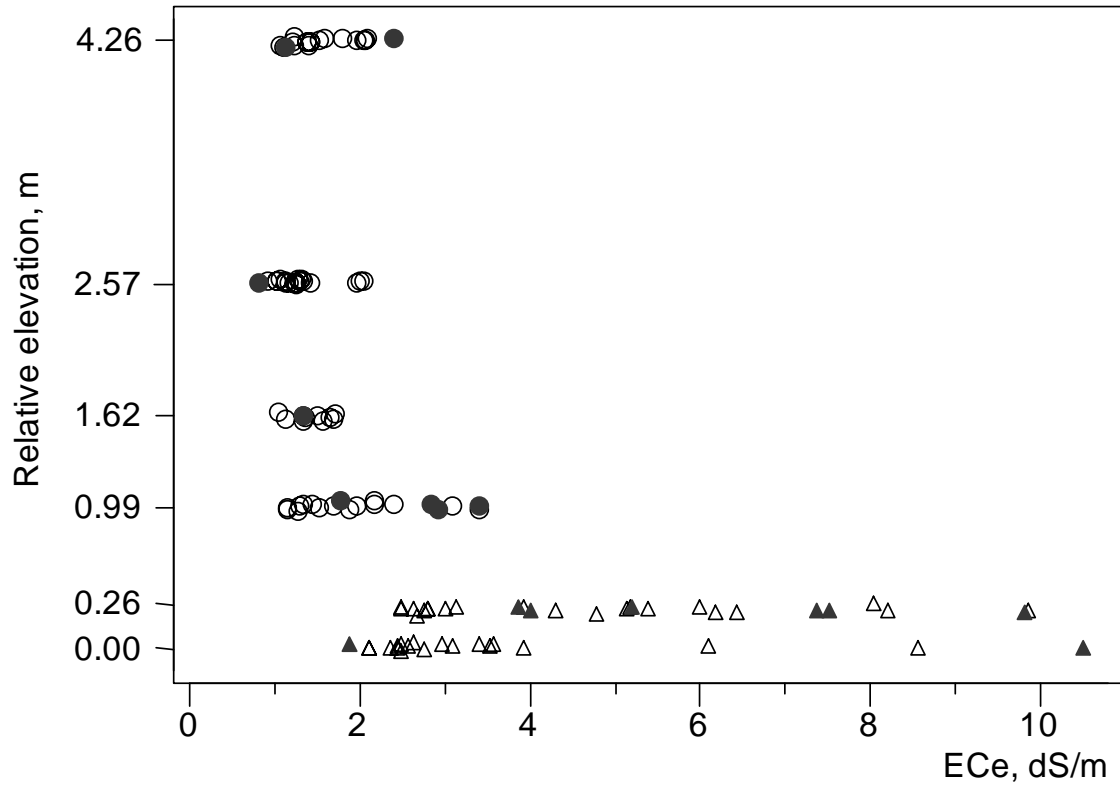
848



849

850 **Figure 2.** Estimates of EC_e from 0 to 50 cm in the 101 EMI reading points (open marks) and
 851 laboratory measured EC_e up to the same depth in 16 of these points (solid marks), against their
 852 relative elevation. Calibration in paddies 1 to 4 (circles) was performed with regression #4, and
 853 in paddies 5 and 6 (triangles) with regression #5 (see Table 2).

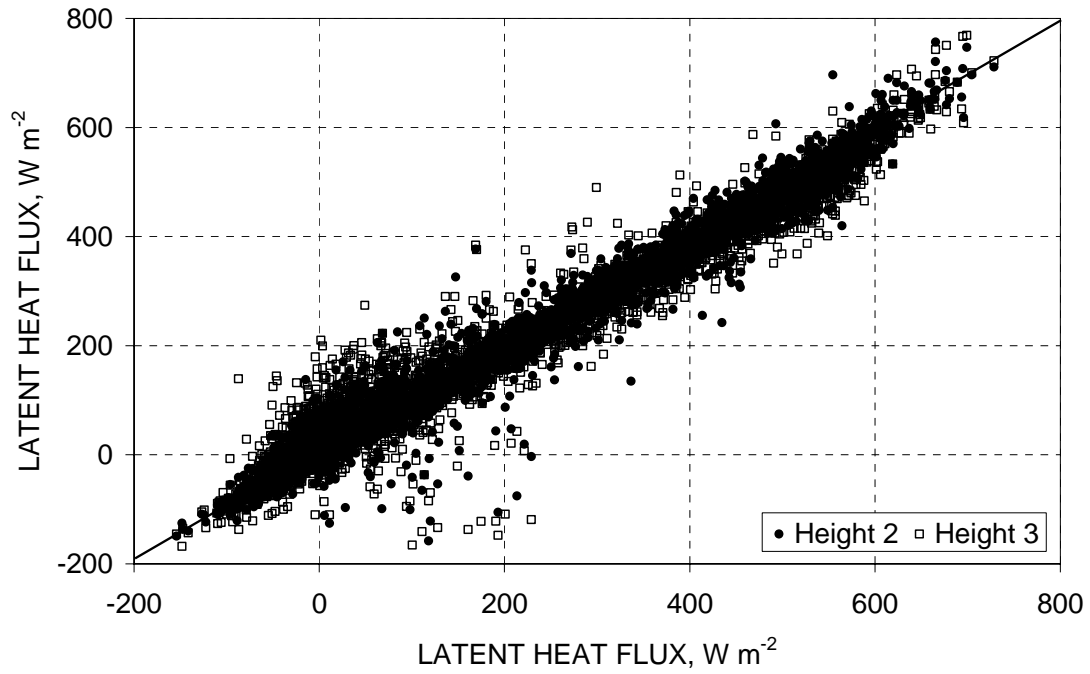
854



855

856 **Figure 3.** Half-hour LE estimates obtained for measurement height 1 (0.5 m above crop canopy,
857 *x*-axis) versus half-hour LE estimates obtained for measurement heights 2 and 3 (0.75 and 1.5
858 m above measurement height 1, respectively) (*y*-axis).

859

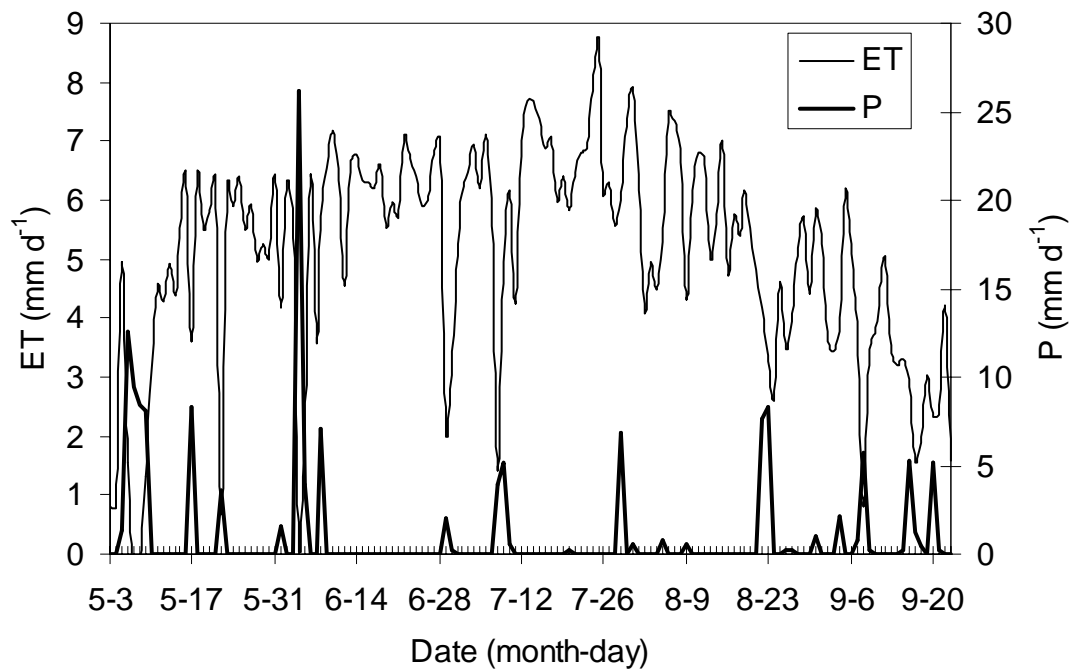


860
861

862 **Figure 4.** *Seasonal evolution of crop evapotranspiration estimates and precipitation*
863 *measurements.*

864

865

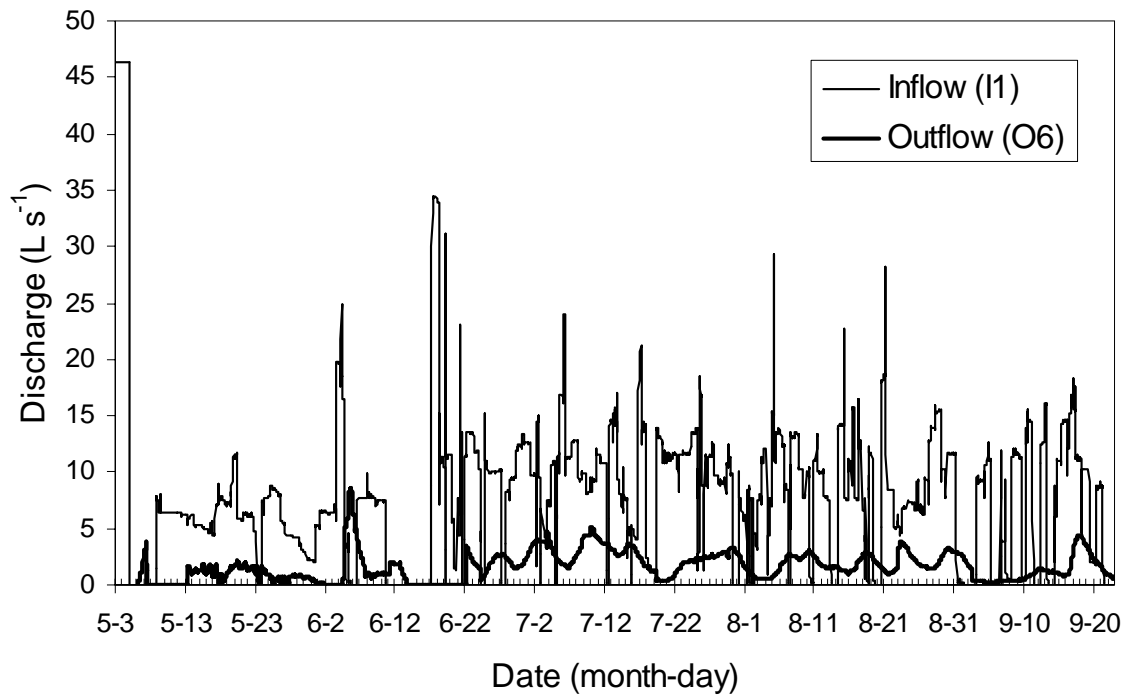


866

867 **Figure 5.** Seasonal evolution of field irrigation inflow (I1) and runoff (O6). The inflow during
868 May 5 and 6 served the purpose of flooding the field. Since the discharge was out of the range of
869 the measuring device, its value was taken from the farmer water order to the irrigation district.

870

871

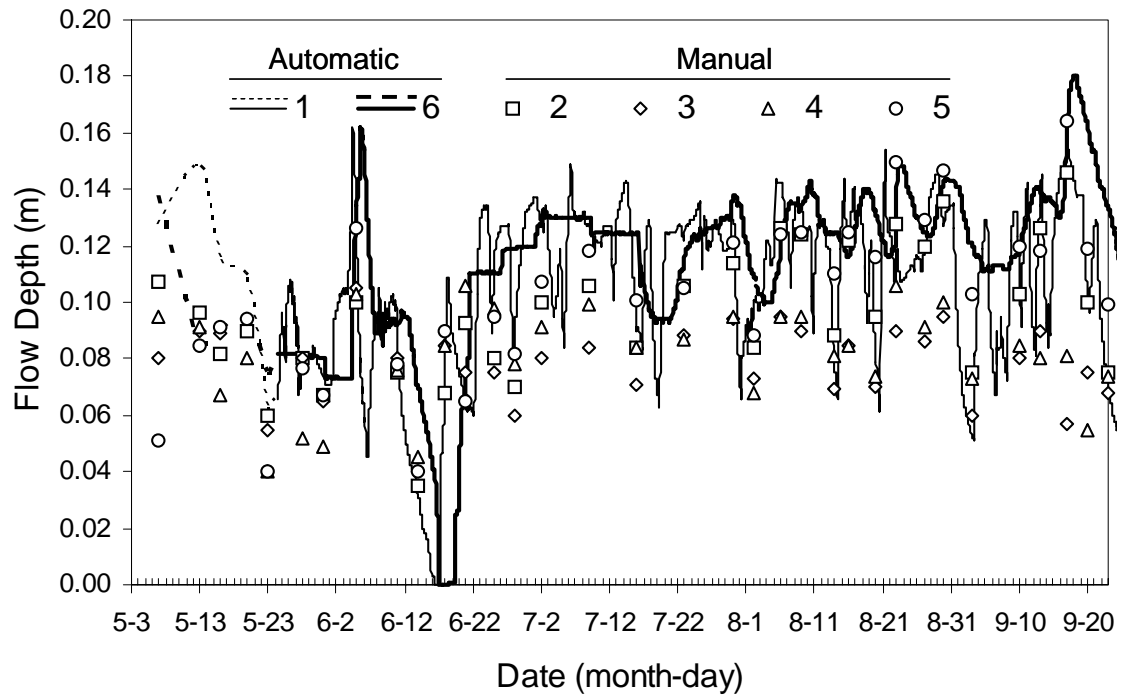


872

873 **Figure 6.** Seasonal evolution of measured flow depth in the paddies. Flow depth was
 874 automatically measured every 30 min in paddies 1 and 6 and manually measured in paddies 2,
 875 3, 4 and 5. Automatic recording started in May 24. Previous values for paddies 1 and 6 were
 876 manually measured (dashed line).

877

878

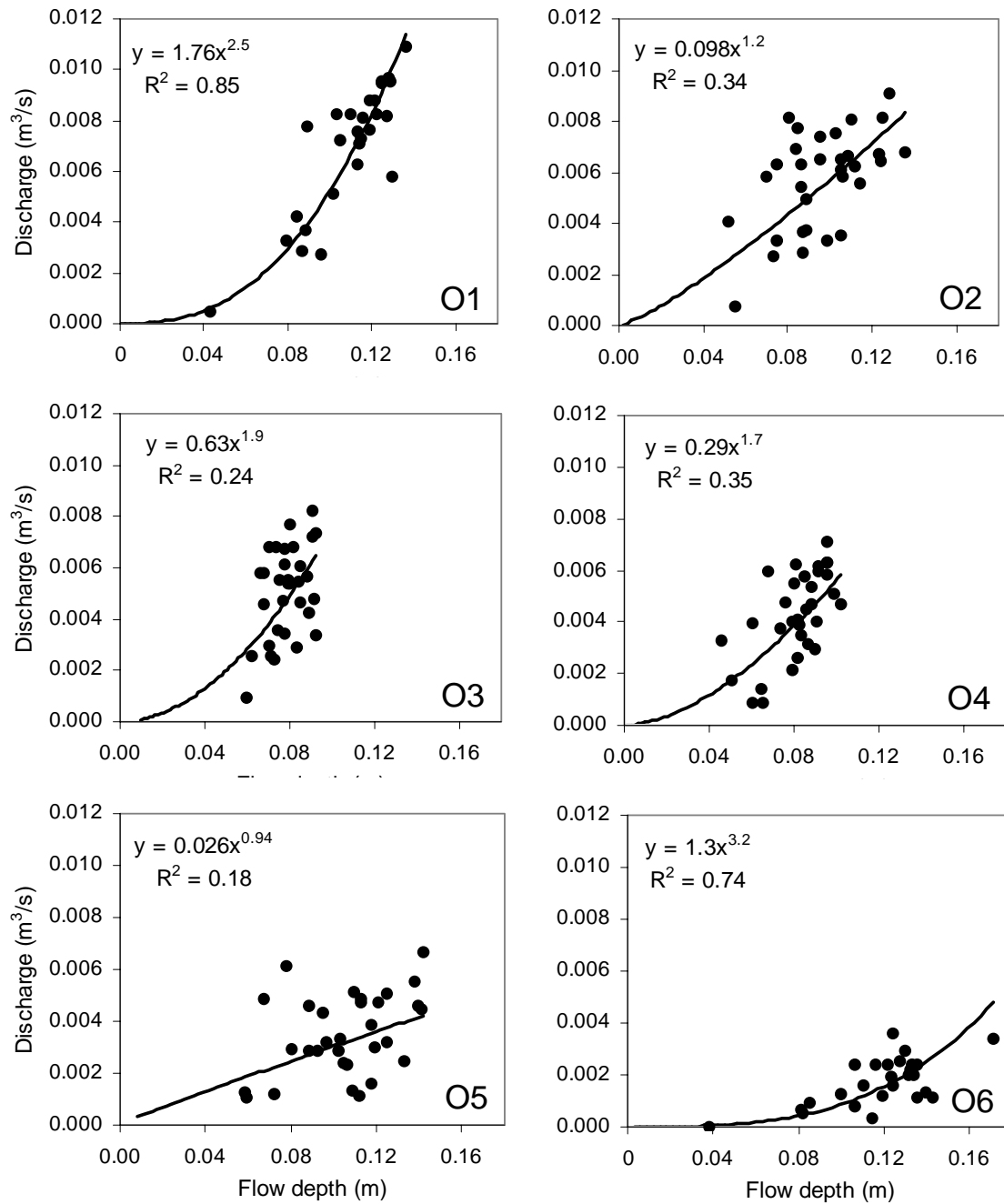


879

880 **Figure 7.** Inter-paddy seasonal flow depth-discharge relationships. Scatter plots, potential
 881 regression lines, regression equations and coefficients of determination are presented for
 882 outflows from paddies 1 to 6.

883

884

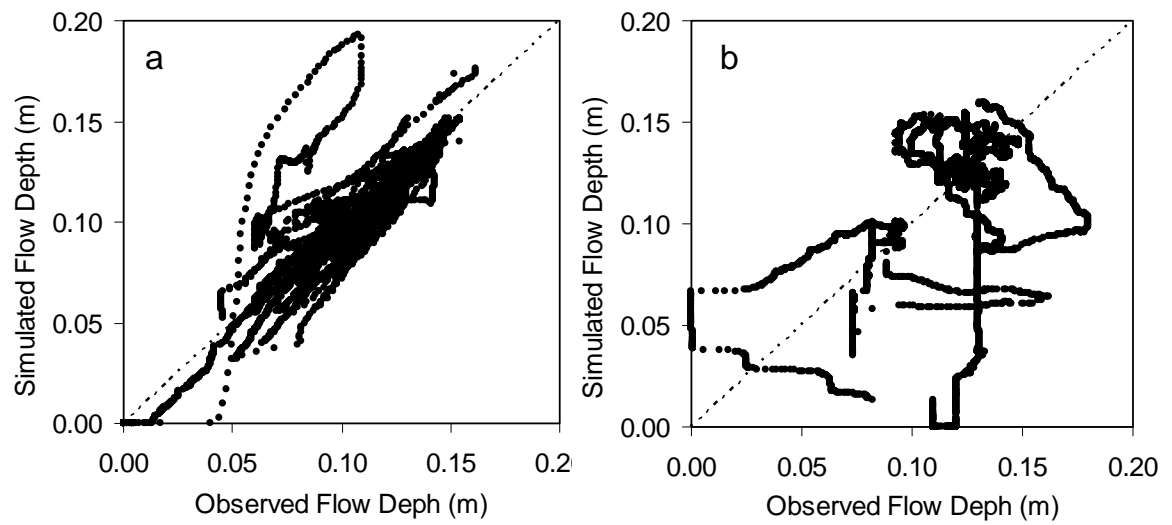


885

886 **Figure 8.** *Observed vs. simulated values of flow depth in paddies 1 (a) and 6 (b).*

887

888

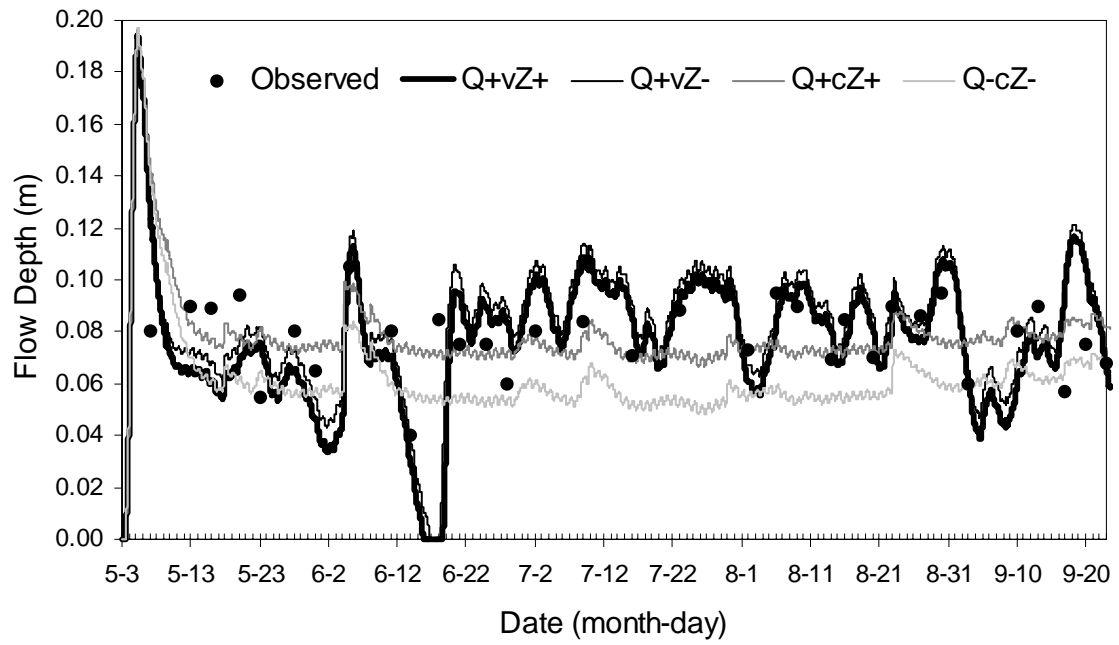


889

890 **Figure 9.** Time evolution of flow depth in Paddy 3 as observed and as simulated for scenarios
891 $Q+vZ+$, $Q+vZ-$, $Q+cZ+$ and $Q-cZ-$.

892

893



894